Fractal counter-current exchange networks

R. S. Farr[1,2] and Y. Mao[3]

[1] *Unilever R&D, Colworth Science Park, Bedford, MK44 1LQ, UK.*
[2] *The London Institute for Mathematical Sciences, 35a South Street, Mayfair, London, UK*
[3] *School of Physics and Astronomy, University of Nottingham, Nottingham, NG7 2RD, UK*

PACS 44.15.+a – Channel and internal heat flow
PACS 05.60.Cd – Classical transport
PACS 47.53.+r – Fractals in fluid dynamics

Abstract – We construct a general analysis for counter-current exchange devices, linking their efficiency to the (potentially fractal) geometry of the exchange surface and supply network. For certain parameter ranges, we show that the optimal exchanger consists of densely packed pipes which span a thin sheet of large area, which may be crumpled into a fractal surface and supplied with a fractal network of pipes. We present the efficiencies of such fractal exchangers, showing factor gains compared to regular exchangers, using parameters relevant for systems such as pigeon lungs and salmon gills.

Introduction. – The design of efficient exchange devices is an important problem in engineering and biology. A wide variety of heat exchangers, such as plate, coil and counter-current, are employed in industrial settings [1], while in nature, leaf venation, blood circulation networks, gills and lungs have evolved to meet multiple physiological imperatives. A distinctive feature of the biological examples is their complex, hierarchical (fractal) nature [2], with branching and usually anastomosing geometries [3, 4]. It is clear that one reason for this is the possibility to include a large surface for exchange within a compact volume (the human lungs for example comprise an alveolar area greater than $50\mathrm{m}^2$ [5]). However, maximal surface area is unlikely to be the only criterion for optimization. For example, West *et al* analysed biological circulatory systems on the basis that power is minimised with the constraint that a minimum flux of respiratory fluid is brought to every cell in the volume of an organism; they were able to explain the well known allometric scaling laws in biology [2].

With the advance of new fabrication technologies such as 3D printing [6], it will become possible to build structures of comparable complexity to biological systems, so there is a need not only to understand in detail the principles and compromises upon which natural systems are based, but also for that understanding to be constructive and accessible, mapping system parameters to actual designs.

The analytical literature in this area has focused on heat transfer from a fluid to a solid body, with a particular emphasis on cooling of integrated circuits [7]. Branching fractal networks are much studied due to their ability to give good heat transfer with a low pressure drop [8,9] (although sometimes simpler geometries can be more efficient [10]), and multiscale structures are also found to have a high heat transfer density [11].

In this Letter, we consider exchange as a general process, which includes gas and heat exchanges, and we look for the optimal designs which can ensure complete exchange (to be defined below) while requiring a minimum amount of mechanical power to generate the necessary fluid flows. We use the language of heat exchange since the relevant material properties have widely used its notation, and gather problem parameters into dimensionless groups, which span the space of possible exchange problems.

Suppose there are two counter-flowing (perhaps dissimilar) fluids with given properties: thermal conductivities κ_j ($j \in \{1, 2\}$), heat capacities per unit volume C_j and viscosities η_j. Let there be an imposed difference ΔT in the *inlet* temperatures, and an imposed volumetric flow rate Q_1 of fluid 1 (while we are free to choose Q_2). The streams are separated by walls of thickness w (taken to be the minimum consistent with biological or engineering constraints) and thermal conductivity κ_{wall} (again an imposed constraint). We assume that the exchanger needs to be compact, in that it fits inside a roughly cubical volume of side length $L_{\max}$, and the pipes are each of length

$L \leq L_{\max}$. Last, we wish the exchange process to go to completion, in that the total exchanged power is of order $E_{\rm end} = C_1 Q_1 \Delta T$. Our aim is to find an exchange network which satisfies all these constraints (which are a typical set for both engineering and biological systems), while requiring the minimum amount of power to drive the flow through the network.

To proceed, we non-dimensionalise on $L_{\max}$ and $\kappa_{\rm wall}$:

$$\hat{w} \equiv w/L_{\max}, \quad \hat{r}_j \equiv r_j/L_{\max}, \quad \hat{L} \equiv L/L_{\max}, \quad \hat{A} \equiv A/L_{\max}^2 \quad \text{and} \quad \hat{\kappa}_j \equiv \kappa_j/\kappa_{\rm wall}.$$

The specification of the problem can be conveniently reduced to three non-dimensional parameters, the first two of which capture the asymmetry of the two fluids:

$$\beta \equiv (C_1/C_2)^2(\eta_2/\eta_1) \quad \text{and} \quad \gamma \equiv \kappa_1/\kappa_2. \tag{1}$$

We note that if all the available volume were filled with pipes of the smallest possible radius, and the two fluids were set to uniform temperatures differing by ΔT, then there would be a maximum possible exchanged power of order $E_{\max} = \Delta T \kappa_{\rm wall} L_{\max}^3/w^2$. Thus our last parameter is the ratio of the required exchange rate to this maximum:

$$\epsilon \equiv E_{\rm end}/E_{\max} = Q_1 C_1 w^2/(L_{\max}^3 \kappa_{\rm wall}), \tag{2}$$

and we typically expect $\epsilon \ll 1$.

Regular exchangers. – To begin, we consider a regular array of counter-flowing streams in N_j straight pipes of radii r_j ($j = 1, 2$) and length L [the same for both types; see fig. 1(b)], where we ignore any feed network to supply the individual pipes. Assuming roughly circular pipes, we approximate the total cross section (perpendicular to flow) of the array as $A \approx \pi N_1 (r_1 + w/2)^2 + \pi N_2 (r_2 + w/2)^2$. Let α be the area across which exchange occurs, then if no clustering of one type occurs α will be approximately the minimum of the two pipe perimeters, multiplied by L. We thus propose the simple approximation to the total area across which exchange occurs:

$$\alpha^{-1} \approx (2\pi L)^{-1} \left[(N_1 r_1)^{-1} + (N_2 r_2)^{-1} \right]. \tag{3}$$

When is exchange complete? We assume the pipes are slender, so that heat diffusion along the length of a pipe is negligible compared to advection, and that the temperature over a cross section perpendicular to its length is roughly uniform. Let z be the distance along a pipe, with $z = 0$ being the upstream end of fluid '1'. Then we have average temperatures $T_j(z)$ over cross sections in each of the two types of pipe. We define $\Delta T \equiv T_1(0) - T_2(L)$. By considering the total heat flux per unit length $J(z)$ between the two sets of pipes, we can write down the material derivative of temperature as each fluid moves along its respective pipe:

$$\pi N_j r_j^2 C_j \frac{DT_j}{Dt} = (-)^j J(z), \tag{4}$$

$$\frac{D}{Dt} \equiv \frac{\partial}{\partial t} + (-)^{j+1} \frac{Q_j}{\pi N_j r_j^2} \frac{\partial}{\partial z}$$

where $j \in \{1, 2\}$, and if s is the thermal conductance per unit area between pipes we find:

$$J(z) \approx \alpha s [T_1(z) - T_2(z)]/L$$

$$s^{-1} \approx (w/\kappa_{\rm wall}) + (r_1/\kappa_1) + (r_2/\kappa_2). \tag{5}$$

In the steady state regime, $\partial/\partial t \equiv 0$ so eqs. (4) lead to an exchanged power E where

$$\frac{E}{s\alpha\Delta T} = \frac{\xi_1 \xi_2 (e^{1/\xi_1} - e^{1/\xi_2})}{\xi_2 e^{1/\xi_1} - \xi_1 e^{1/\xi_2}} \approx \min(1, \xi_1, \xi_2) \tag{6}$$

$$\xi_j \equiv Q_j C_j/(s\alpha). \tag{7}$$

Complete exchange means $E \approx C_1 Q_1 \Delta T$, which from eqn. (6) means $\xi_1 \leq \xi_2$ and $\xi_1 \leq 1$. We note from the analysis accompanying eq. (6) that there is a special case of a 'balanced' exchanger, in which $Q_1 C_1 = Q_2 C_2$ (so $\xi_1 = \xi_2$) and the change of temperature with z for both streams is linear, rather than being exponential. The optimal exchanger should have this property, since otherwise some of the pipe length will contribute to dissipated power but not exchange.

Now we seek to minimise the total power P required to run the exchanger, $P = Q_1 \Delta p_1 + Q_2 \Delta p_2$, where Δp_j are the pressures dropped across the two types of pipes. For laminar (Poiseuille) flow, and using the 'balanced' condition $Q_1 C_1 = Q_2 C_2$ to eliminate Q_2, we obtain:

$$P = P_0 \hat{L} \left(\frac{1}{N_1 \hat{r}_1^4} + \frac{\beta}{N_2 \hat{r}_2^4} \right), \tag{8}$$

$$P_0 \equiv 8 Q_1^2 \eta_1/(\pi L_{\max}^3).$$

Our task is to minimise P in eq. (8) by choosing the five quantities N_j, $\hat{r}_j$ and $\hat{L}$, while also ensuring the exchanger is compact (fits in the required volume):

$$\max(\hat{r}_j) \leq \hat{L} \leq 1, \tag{9}$$

$$\hat{A} = \pi N_1 (\hat{r}_1 + \hat{w}/2)^2 + \pi N_2 (\hat{r}_2 + \hat{w}/2)^2 \leq 1, \tag{10}$$

and also that exchange is complete, which from $\xi_1 \leq 1$ and eqs. (3), (5), (7) leads to

$$\epsilon \left(\hat{w} + \frac{\hat{r}_1}{\hat{\kappa}_1} + \frac{\hat{r}_2}{\hat{\kappa}_2} \right) \left(\frac{1}{N_1 \hat{r}_1} + \frac{1}{N_2 \hat{r}_2} \right) \leq 2\pi \hat{L} \hat{w}^2. \tag{11}$$

The optimization can then be performed numerically by a simple downhill search. Table 1 shows the geometry of some optimised regular exchangers for real cases, and the optimised results are included in fig. 3 with the label 'regular'.

Branched supply network. – Now, consider the branched (and fractal) supply network shown in fig. 1(c), which brings the streams to the exchanger ('active layer'). In contrast to Ref. [2], we do not need the supply network to pass close to every point in space; we only require that it does not dominate the power dissipated in driving the

System:	T.E.G.	Pigeon	Salmon
Exchanged:	Heat	Oxygen	Oxygen
$L_{\max}$/m	$2.0\ 10^{-1}$	$5.0\ 10^{-2}$	$2.0\ 10^{-2}$
w/m	$5.0\ 10^{-4}$	$5.0\ 10^{-7}$	$5.0\ 10^{-7}$
$Q_1/\mathrm{m^3 s^{-1}}$	$5.0\ 10^{-2}$	$2.0\ 10^{-5}$	$1.0\ 10^{-6}$
C_1/S.I.	$1.0\ 10^{3}$	$2.0\ 10^{-6}$	$2.0\ 10^{-6}$
C_2/S.I.	$1.0\ 10^{3}$	$1.3\ 10^{-5}$	$1.0\ 10^{-7}$
κ_1/S.I.	$4.0\ 10^{-2}$	$1.8\ 10^{-16}$	$1.6\ 10^{-16}$
κ_2/S.I.	$4.0\ 10^{-2}$	$2.3\ 10^{-10}$	$1.6\ 10^{-16}$
κ_{wall}/S.I.	$1.0\ 10^{1}$	$1.8\ 10^{-16}$	$1.6\ 10^{-16}$
η_1/Pa s	$4.0\ 10^{-5}$	$4.0\ 10^{-3}$	$4.0\ 10^{-3}$
η_2/Pa s	$4.0\ 10^{-5}$	$4.0\ 10^{-5}$	$1.0\ 10^{-3}$
β	$1.0\ 10^{0}$	$2.4\ 10^{-4}$	$1.0\ 10^{2}$
γ	$1.0\ 10^{0}$	$7.8\ 10^{-7}$	$1.0\ 10^{0}$
ϵ	$1.6\ 10^{-4}$	$4.4\ 10^{-4}$	$3.9\ 10^{-4}$
$r_{1,\mathrm{reg}}$/m	$1.0\ 10^{-3}$	$2.5\ 10^{-5}$	$5.2\ 10^{-6}$
$r_{2,\mathrm{reg}}$/m	$1.0\ 10^{-3}$	$2.2\ 10^{-6}$	$2.1\ 10^{-5}$
$A_{\mathrm{reg}}/\mathrm{m^2}$	$4.0\ 10^{-2}$	$2.5\ 10^{-3}$	$4.0\ 10^{-4}$
L_{reg}/m	$2.0\ 10^{-1}$	$5.0\ 10^{-2}$	$2.0\ 10^{-2}$
P_{reg}/W	$2.4\ 10^{1}$	$6.2\ 10^{-1}$	$7.7\ 10^{-1}$
$r_{1,\mathrm{frac}}$/m	$5.1\ 10^{-4}$	$5.0\ 10^{-6}$	$5.0\ 10^{-6}$
$r_{2,\mathrm{frac}}$/m	$5.1\ 10^{-4}$	$5.4\ 10^{-7}$	$7.1\ 10^{-6}$
$A_{\mathrm{frac}}/\mathrm{m^2}$	$6.6\ 10^{-2}$	$1.0\ 10^{-2}$	$7.7\ 10^{-4}$
L_{frac}/m	$4.4\ 10^{-2}$	$7.1\ 10^{-4}$	$2.8\ 10^{-3}$
P_{frac}/W	$1.8\ 10^{1}$	$6.0\ 10^{-2}$	$4.0\ 10^{-1}$

Table 1: Estimated parameters for various real systems. 'S.I.' refers to the international system of units; so for thermal systems C will have units $\mathrm{Jm^{-3}K^{-1}}$ and κ will have units $\mathrm{Wm^{-1}K^{-1}}$. For gas exchange, C will have units kilogram of relevant gas per $\mathrm{m^3}$ of fluid, per Pascal of partial pressure, and κ will have units $\mathrm{kg\,s^{-1}m^{-1}Pa^{-1}}$ (so that κ/C is a diffusivity). 'T.E.G.' is thermo-electric generation from internal combustion engine exhaust (we have chosen values corresponding to a car/personal automobile). For the animal respiratory systems we assume that transport across the exchange membrane is similar to that of water. For blood, we assume that oxygen can exist in a mobile form (dissolved in the water-like serum) and an immobile form (bound to haemoglobin). Thus the oxygen conductivity κ_1 for blood is the same as for water, while C_1 is increased over that of water by the carrying capacity of haem. Data are from Refs. [14–18]. Results for a regular exchange network are indicated by the subscript 'reg'; while the results for the fractal exchange surfaces (denoted by a subcript 'frac') use a Hausdorff dimension $d = 2.33$. For the cases of pigeon and salmon respiration, we impose the additional constraint that $r_1 > 5\mu$m, in order to allow erythrocytes to pass through. This only affects the fractal case, and without this requirement, the optimised value of r_1 for the fractal case would be 1.5μm and 0.4μm respectively.

exchanger. Suppose that the pipes comprising the supply network branch into b smaller pipes at each hierarchical level k of the tree, (where pipes with higher values of k are smaller, and closer to the active layer – the regular array of pipes – where exchange occurs). Let the ratio of pipe radii between neighbouring levels be $\rho < 1$, and the ratio of pipe lengths be λ. The ratio of power dissipated between hierarchical levels is therefore

$$P_{k+1}/P_k = \lambda/(b\rho^4). \tag{12}$$

Since the active layer is densely covered with pipes, the condition to fit the supply network into space is $\rho \geq b^{-1/2}$. Therefore, provided $\lambda > b\rho^4$, the power will increase exponentially with k and the overall power dissipation in the supply network will be of order that in the last layer; and therefore of the same order as in the active layer. The supply network will therefore not dominate the power dissipation.

Double fractal exchange networks. – From the solutions to the optimum regular exchange networks, the lateral cross section A always expands to its maximum value $L^2_{\max}$. If this restriction were lifted, a more efficient exchanger would likely be possible. This can be achieved by allowing the active layer (provided it is thin enough, and can still be provided with a branching supply network) to become corrugated, while still fitting within the prescribed roughly cubical volume $L^3_{\max}$ available. One way to do this is to turn the active layer into an approximation to a fractal surface. Suppose the active layer is corrugated into a fractal surface over a range of lateral length scales down to a scale $x \geq L$, such that in the limit $x \to 0$ the Hausdorff dimension [19] of the surface would be d. Fig. 2 shows schematically an example in which the surface is the type I quadratic Koch surface with (in the limit) Hausdorff dimension $d_{\mathrm{koch}} = \ln 13/\ln 3 \approx 2.33$. Let the area of the active layer be $A(x)$, where $A(L_{\max}) = L^2_{\max}$, then from Hausdorff's definition of dimension, we see that $A(x) = L^2_{\max}(x/L_{\max})^{2-d}$. We can therefore replace the inequality $\hat{A} \leq 1$ in eq. (10) by

$$\hat{A} = \pi N_1(\hat{r}_1 + \hat{w}/2)^2 + \pi N_2(\hat{r}_2 + \hat{w}/2)^2 \leq \hat{L}^{2-d}. \tag{13}$$

Fig. 3 shows the effect of ϵ (varied through altering Q_1) on the power dissipation for fractal exchangers corresponding to the scenarios in table 1, compared to that of the regular exchanger. Corrugating the exchange layer into a type I quadratic Koch surface leads to a significant reduction in the dissipated power for the two biological cases (factor gain of 10 for pigeon lungs and 2 for salmon gills). However, the small size of the optimum pipe radii r_1 may mean that this degree of optimization is precluded by other considerations. For instance, erythrocytes need to be able to pass through these type 1 (blood carrying) vessels.

Conclusions. – Exchange networks of the class we show here exhibit broadly power-law dependence of the dissipated power with the quantity ϵ (which measures the required throughput: the rate of exchange of heat or gas needed). This is true both for a fractally corrugated or a simple regular array of exchange pipes. However, the fractal exchangers demonstrate factor gain in efficiency when compared to regular exchangers for parameters relevant

for pigeon lungs and salmon gills. The exchangers exhibit a crossover between regimes as a function of the required throughput, where different constraints (geometrical or completeness of exchange) are limiting; and if other parameters were changed, such as conductivities, one could expect regimes in which either wall or fluid conductivity would be limiting.

We note that the analysis we have performed here aims specifically to minimise required power while ensuring complete exchange has taken place. In practice, other design constraints may need to be included, for example a requirement that the network be robust [3] or repairable [20, 21] under external attack [22, 23], or the cost of building the network may be significant compared to its operating costs [24, 25].

REFERENCES

[1] Green D.W. and Perry R.H. (Editor), *Perry's Chemical Engineers' Handbook, Eighth Edition* (McGraw-Hill) 2007.

[2] West G., Brown J.H. and Enquist B.J., *Science*, **276(5309)** (1997) 122.

[3] Katifori E., Szöllösi G.J and Magnasco M.O., *Phys. Rev. Lett.*, **104** (2010) 048704.

[4] Makanya A.N and Djonov V., *Microscopy Research and Technique*, **71(9)** (2008) 689.

[5] Wiebe B.M. and Laursen H., *Microscopy Research and Technique*, **32** (1995) 255.

[6] Hague R. and Reeves P., *Ingenia*, **55** (2013) 38.

[7] Tuckerman D.B. and Pease R.F.W., *Electron device letters*, **2(5)** (1981) 126.

[8] Bejan A. and Errera M.R., *Fractals*, **5(4)** (1997) 685.

[9] Chen Y. and Cheng P., *Int. J. Heat and Mass Transfer*, **45** (2002) 2643.

[10] Escher W., Michel B. and Poulikakos D., *Int. J. Heat and Mass Transfer*, **52(5-6)** (2009) 1421.

[11] Bejan A. and Fautrelle Y., *Acta Mechanica*, **163(1-2)** (2003) 39.

[12] Twigg M.V., *Applied Catalysis B: Environmental*, **70** (2007) 2.

[13] Hagenbach E., *Annalen der Physik und Chemie*, **109** (1860) 385.

[14] Lide D.R. (Editor), *Handbook fo chemistry and physics, 75th Edn* (CRC Press, Inc.) 1995.

[15] *Diffusion: Mass Transfer in Fluid Systems (2nd ed.)* Cussler E.L., (Cambridge University Press) 1997.

[16] *Animal physiology: adaptation and environment* Schmidt-Nielsen K., (Cambridge University Press, Cambridge) 1990.

[17] Butler P.J., West N.H. and Jones D.R., *Journal of Experimental Biology*, **71** (1977) 7.

[18] Kicenuik J.W. and Jones D.R., *Journal of Experimental Biology*, **69** (1977) 247.

[19] Hausdorff F., *Mathematische Annalen*, **79(1-2)** (1919) 157.

[20] Quattrociocchi W., Caldarelli G. and Scala A., *PLoS ONE*, **9(2)** (2014) e87986.

[21] Farr R.S., Harer J.L. and Fink T.M.A., *Phys. Rev. Lett.*, **113(3)** (2014) 138701.

[22] Cohen R., Erez K., ben-Avraham D. and Havlin S., *Phys. Rev. Lett.*, **85** (2000) 4626.

[23] Cohen R., Erez K., ben-Avraham D. and Havlin S., *Phys. Rev. Lett.*, **86** (2001) 3682.

[24] Bohn S. and Magnasco M.O., *Phys. Rev. Lett.*, **98** (2007) 088702.

[25] Durand M., *Phys. Rev. Lett.*, **98** (2007) 088701.

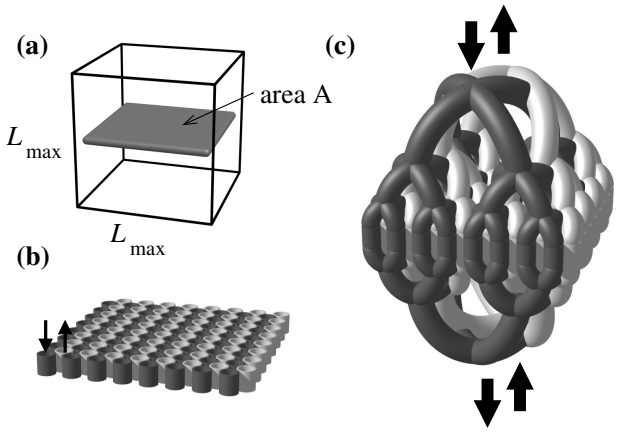

Fig. 1: (a) Schematic of the geometry of a counter-current heat exchanger ('active layer') fitting inside a prescribed cubic volume of side length $L_{\max}$. (b) Detail of the active layer, showing a regular array of pipes carrying alternately counter-flowing streams. (c) The active layer connected to a branching and (on the other side) anastomosing fractal supply network.

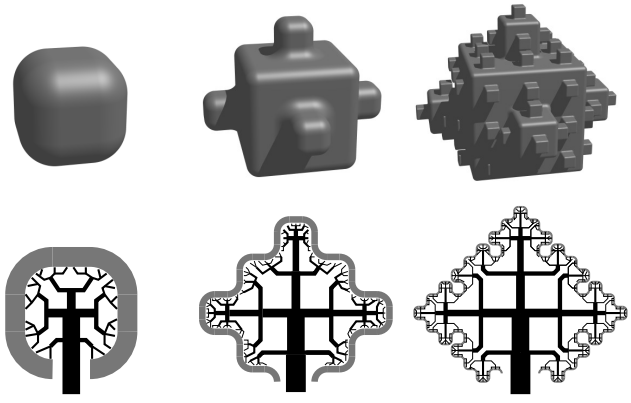

Fig. 2: Top row: schematic of the active layer of fig. 1(a), corrugated into a hierarchical (fractal) surface, comprising (left to right) greater area and more iterations of the fractal. Bottom row: Schematic section through these surfaces showing the fractal supply network in the interior (the corresponding network outside is not shown, and will require a more complex design to ensure equal flow to all parts of the active layer).

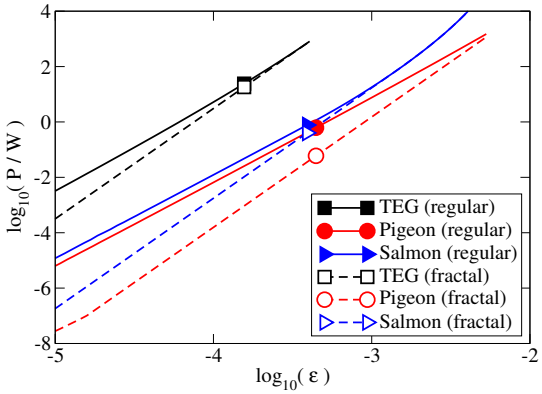

Fig. 3: Plots of power dissipated in exchange for the three cases of table 1. Here we change Q_1 to achieve different values of ϵ. The actual cases in table 1 are shown as symbols, and for some cases, a change of regime is observed, witnessed by a change in the slope of the line; although the curve visible in the top right part of the curve for 'Salmon (fractal)' are due to the constraint that blood vessels (type 1 pipes) should be large enough to carry erythrocytes (taken as the condition $r_1 > 5\mu$m).